Journal of Computational and Applied Mathematics 234 (2010) 1842–1850

Contents lists available at ScienceDirect

Journal of Computational and Applied Mathematics

journal homepage: www.elsevier.com/locate/cam

Reflection and transmission by a slab with randomly distributed isotropic point scatterers

Agnès Maurel

Laboratoire Ondes et Acoustique, UMR CNRS 7587, Ecole Supérieure de Physique et de Chimie Industrielles, 10 rue Vauquelin, 75005 Paris, France

ARTICLE INFO

Article history:
Received 3 December 2007
Received in revised form 12 May 2008

Keywords:
Multiple scattering
Random media
Reflection & transmission

ABSTRACT

The problem of how a wave propagates in an infinite medium filled with scatterers has revealed the notion of an effective medium: the mean wave propagates as in an homogeneous medium with complex index. Is this notion of an effective medium still valid when the scatterers are bounded in space? The problem is treated here for isotropic point scatterers. It is shown that (i) the waves propagate inside the slab with an effective wavenumber K being the same as that in an infinite medium, (ii) the reflection and transmission coefficients of the slab mainly behave as $R \simeq (1-e^{iKL})(k-K)/2k$ and $T \simeq e^{iKL}$ at leading order, (iii) the reflection and transmission coefficients of a single interface are related to R and T with the usual law of optics and (iv) the boundary conditions to be applied at the interface are the continuity of the field and its first derivative for isotropic scatterers. Finally, numerical experiments in one dimension show satisfactory agreement with the presented theory.

1. Introduction

The problem of multiple scattering by randomly distributed scatterers has been widely studied and a large part of the literature is devoted to the derivation of the index of the so-called effective medium. This medium corresponds to a fictitious homogeneous dissipative medium felt by the "mean", or coherent, acoustic wave when it propagates, the coherent wave being the wave averaged over all realizations of the scatterer configurations, such as their positions and their characteristics. These studies have attracted considerable interest because of their practical applications from at least two domains: the geophysics literature seeks to understand the effect of inhomogeneities within the Earth's crust on seismic waves [1,2] and the non-destructive evaluation literature seeks to gauge the effect that flaws in elastic materials have on elastic waves [3].

Until recently, most of the studies on the properties of the coherent wave focused on the determination of the complex index only. However, questions that reasonably arise are: (1) Does the multiple scattering medium still behave as a homogeneous (effective) medium when the scatterers occupy a bounded region of the space only? In the case of a slab of finite width, the questions are for instance whether or not the forward mean wave still propagates with an effective wavenumber, whether or not the backward mean wave propagates with the same wavenumber, and (2) if yes, what are the boundary conditions to be applied at the fictitious interface between the homogeneous effective medium and the homogeneous medium free of scatterers? Over the past 10 years, there has been an increasing response to both questions (1) and (2). In addition to the fundamental interest in the notion of an effective medium and whether or not this notion is robust, motivations come from practical situations in which the coherent backward wave is available (see e.g. [4]). Many studies have extended Foldy's method to the problem of a slab of finite width, yielding predictions on the reflection and transmission properties in two dimensions [5–7] and in three dimensions [8,9], including or not the finite size of

E-mail address: agnes.maurel@espci.fr.

0377-0427/$ – see front matter
doi:10.1016/j.cam.2009.08.035

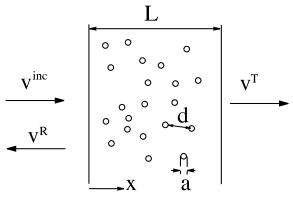

Fig. 1. Slab of finite width L filled with randomly distributed scatterers of characteristic size a (with volume $\mathcal{V}_s$), with a filling fraction $\varphi \equiv \mathcal{V}_s/d^D$. The incident wave in free space has a wavenumber k. The slab can be one, two or three dimensions (in two and three dimensions, the calculations are restricted to the case of incidence normal to the "fictitious" interfaces).

the scatterers. Furthermore, following Berryman's work, homogenization techniques have been used to characterize the reflection and transmission properties of a periodic set of scatterers in terms of effective parameters [10,11].

In the present paper, we adopt an alternative method avoiding Foldy's approach that is known to use an unjustified closure assumption (see also [12]). To do that, the total field v scattered by an ensemble of randomly placed scatterers is written in the second Born approximation to get an explicit expression of the mean field $\langle v \rangle$. An expansion for small scatterer size is then performed. In the resulting expansion, terms up to $O(\epsilon^2)$ and $O[(ka)^2]$ are retained. The limitations of the study are: (i) the scatterers are assumed to be of small size $ka \to 0$ and (ii) the ϵ-parameter, in which the expansion is performed, implies weak scattering strength. Finally, the present approach is not free of criticism because of the non-uniformity that might arise in the Born expansion. That is, the expansions are in principle valid only for short propagation distances. To increase the range of validity of this expansion, renormalization techniques are used, the simplest one being the one used in the present study (see [13] and the references herein).

2. Effective wave field in the limit of point scatterers

We consider a distribution of N scatterers, in dimension $D = 1, 2$ or 3, with a size a randomly distributed in a region sandwiched between $x = 0$ and $x = L$ as pictured in Fig. 1. The region inside the scatterer centered at $\mathbf{r}_i$ is denoted by $\mathcal{D}_i$ (with volume $\mathcal{V}_s$). The effect of the scatterers is embedded in a potential V written as in the right-hand side term of the wave equation (see Eq. (1)). The propagation of the wave is described by the wave equation

$$\Delta v(\mathbf{r}) + k^2 v(\mathbf{r}) = V(\mathbf{r}) v(\mathbf{r}), \qquad V(\mathbf{r}) = k^2 \sum_i \epsilon_i \Pi_a(\mathbf{r} - \mathbf{r}_i), \tag{1}$$

where $\Pi_a(\mathbf{r}) = 0$ for $\mathbf{r} \notin \mathcal{D}_i$ and $\Pi_a(\mathbf{r}) = 1$ for $\mathbf{r} \in \mathcal{D}_i$, ϵ_i is a small parameter that accounts for the small scattering strength, k is the wavelength of the incident wave, and $\mathbf{r}_i$ is the position vector of the i-th scatterer. Typically, for a scatterer with a contrast in the sound speed from c_i inside the i-th scatterer to c in the background medium, Eq. (1) applies with $\epsilon_i = 1 - c_i^2/c^2$.

For clarity, we now use non-dimensional quantities $\tilde{\mathbf{r}} \equiv k\mathbf{r}$, and Eq. (1) becomes

$$\Delta v(\tilde{\mathbf{r}}) + v(\tilde{\mathbf{r}}) = \sum_i \epsilon_i \Pi_{ka}(\tilde{\mathbf{r}} - \tilde{\mathbf{r}}_i). \tag{2}$$

Using the Green function G^0 in the free space, which satisfies $(\Delta + 1)G^0(\tilde{\mathbf{r}}) = \delta(\tilde{\mathbf{r}})$, the integral representation for $v(\tilde{\mathbf{r}})$ is

$$v(\tilde{\mathbf{r}}) = v^{\mathrm{inc}}(\tilde{\mathbf{r}}) + \sum_i \epsilon_i \int_{\tilde{\mathcal{D}}_i} \mathrm{d}\tilde{\mathbf{r}}' G^0(\tilde{\mathbf{r}} - \tilde{\mathbf{r}}') v(\tilde{\mathbf{r}}'), \tag{3}$$

with $\tilde{\mathcal{D}}_i$ the region in the $k\mathbf{r}$-space corresponding to $\mathcal{D}_i$. Expanding the expression of the field v in Eq. (3) to second order in ϵ gives

$$v(\tilde{\mathbf{r}}) = v^{\mathrm{inc}}(\tilde{\mathbf{r}}) + \sum_i \epsilon_i \int_{\tilde{\mathcal{D}}_i} \mathrm{d}\tilde{\mathbf{r}}' G^0(\tilde{\mathbf{r}} - \tilde{\mathbf{r}}') v^{\mathrm{inc}}(\tilde{\mathbf{r}}') + \sum_i \sum_j \epsilon_i \epsilon_j \int_{\tilde{\mathcal{D}}_i} \mathrm{d}\tilde{\mathbf{r}}' G^0(\tilde{\mathbf{r}} - \tilde{\mathbf{r}}') \int_{\tilde{\mathcal{D}}_j} \mathrm{d}\tilde{\mathbf{r}}'' G^0(\tilde{\mathbf{r}}' - \tilde{\mathbf{r}}'') v^{\mathrm{inc}}(\tilde{\mathbf{r}}'') + O(\epsilon^3). \tag{4}$$

The limit $ka \to 0$ of Eq. (4) involves three integrals; two of them are easily derived:

$$\begin{aligned} &\lim_{ka\to 0} \int_{\tilde{\mathcal{D}}_i} \mathrm{d}\tilde{\mathbf{r}}' G^0(\tilde{\mathbf{r}} - \tilde{\mathbf{r}}') v^{\mathrm{inc}}(\tilde{\mathbf{r}}') = \mathcal{V} G^0(\tilde{\mathbf{r}} - \tilde{\mathbf{r}}_i) v^{\mathrm{inc}}(\tilde{\mathbf{r}}_i) \left[1 + O[(ka)^2]\right], \\ &\lim_{ka\to 0} \int_{\tilde{\mathcal{D}}_i} \mathrm{d}\tilde{\mathbf{r}}' G^0(\tilde{\mathbf{r}} - \tilde{\mathbf{r}}') \int_{\tilde{\mathcal{D}}_{j\neq i}} \mathrm{d}\tilde{\mathbf{r}}'' G^0(\tilde{\mathbf{r}}' - \tilde{\mathbf{r}}'') v^{\mathrm{inc}}(\tilde{\mathbf{r}}'') = \mathcal{V}^2 G^0(\tilde{\mathbf{r}} - \tilde{\mathbf{r}}_i) G^0(\tilde{\mathbf{r}}_i - \tilde{\mathbf{r}}_j) v^{\mathrm{inc}}(\tilde{\mathbf{r}}_j) \left[1 + O[(ka)^2]\right], \end{aligned} \tag{5}$$

where $\mathcal{V} = k^D \mathcal{V}_s$ is the volume of $\tilde{\mathcal{D}}_i$, ($\mathcal{V} = O(ka)$ in one dimension, $O[(ka)^2]$ in two dimensions and $O[(ka)^3]$ in three dimensions). Note that we have used $\int_{\tilde{\mathcal{D}}_i} \mathrm{d}\tilde{\mathbf{r}}'(\tilde{\mathbf{r}}' - \tilde{\mathbf{r}}_i) = \mathbf{0}$ with $\tilde{\mathbf{r}}_i$ the barycenter of $\tilde{\mathcal{D}}_i$. The limit of the third integral is taken

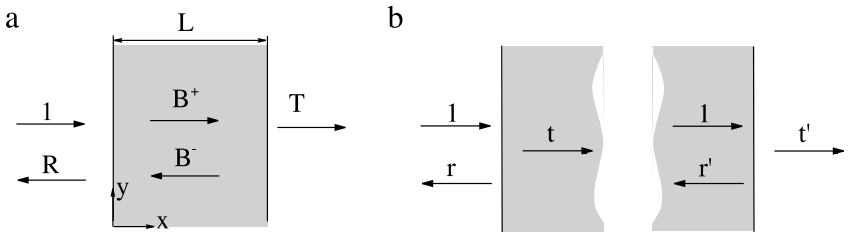

Fig. 2. A region (a slab (a) or single interfaces (b)) filled with scatterers is sought as an effective medium.

by expanding $v^{\text{inc}}(\tilde{\mathbf{r}}'')$ and $G^0(\tilde{\mathbf{r}}-\tilde{\mathbf{r}}')$ in a neighborhood of $\tilde{\mathbf{r}}_i$, both functions having continuous partial derivatives in $\tilde{\mathcal{D}}_i$:

$$\lim_{ka\to 0}\int_{\tilde{\mathcal{D}}_i} \mathrm{d}\tilde{\mathbf{r}}' G^0(\tilde{\mathbf{r}}-\tilde{\mathbf{r}}')\int_{\tilde{\mathcal{D}}_i} \mathrm{d}\tilde{\mathbf{r}}'' G^0(\tilde{\mathbf{r}}'-\tilde{\mathbf{r}}'')v^{\text{inc}}(\tilde{\mathbf{r}}'') = G^0(\tilde{\mathbf{r}}-\tilde{\mathbf{r}}_i)v^{\text{inc}}(\tilde{\mathbf{r}}_i)\lim_{ka\to 0}\int_{\tilde{\mathcal{D}}_0} \mathrm{d}\tilde{\mathbf{r}}'\mathrm{d}\tilde{\mathbf{r}}'' G^0(\tilde{\mathbf{r}}'-\tilde{\mathbf{r}}'')\left[1+O(ka)\right], \tag{6}$$

with $\tilde{\mathcal{D}}_0$ the region for $k\mathbf{r}$ with $\mathbf{r}$ inside a scatterer centered at the origin. The integral $g \equiv \lim_{ka\to 0}\int_{\tilde{\mathcal{D}}_0} \mathrm{d}\tilde{\mathbf{r}}\mathrm{d}\tilde{\mathbf{r}}' G^0(\tilde{\mathbf{r}}-\tilde{\mathbf{r}}')$ can be shown to be divergence free in one dimension, two dimensions and three dimensions. It can be written as $g = \mathcal{V}^2 G^0(kb)$, with b scaling on a: in one dimension, we get $b = a$. In two dimensions, the same result $b = a$ has been shown for cylindrical scatterers in [12]. Depending on the geometry of the scatterer and on the form of the potential V that describes the microscopy of the scatterer (here, we have chosen a step function potential), the relation between b and a can change, but we expect $b \sim a$ in all cases. In the limit $ka \to 0$, the wave field is, from Eq. (4),

$$\begin{aligned} v(\tilde{\mathbf{r}}) = {} & v^{\text{inc}}(\tilde{\mathbf{r}}) + \mathcal{V}\sum_i \epsilon_i G^0(\tilde{\mathbf{r}}-\tilde{\mathbf{r}}_i)v^{\text{inc}}(\tilde{\mathbf{r}}_i)\left[1+O[(ka)^2]\right] + \mathcal{V}^2 G^0(kb)\sum_i \epsilon_i^2 G^0(\tilde{\mathbf{r}}-\tilde{\mathbf{r}}_i)v^{\text{inc}}(\tilde{\mathbf{r}}_i)\left[1+O(ka)\right] \\ & + \mathcal{V}^2\sum_i\sum_{j\neq i}\epsilon_i\epsilon_j G^0(\tilde{\mathbf{r}}-\tilde{\mathbf{r}}_i)G^0(\tilde{\mathbf{r}}_i-\tilde{\mathbf{r}}_j)v^{\text{inc}}(\tilde{\mathbf{r}}_j)\left[1+O[(ka)^2]\right] + O(\epsilon^3). \end{aligned} \tag{7}$$

Note that the term $G^0(kb)$ is related to the so-called "self-irradiation". For a single scatterer located at $\mathbf{r}_i = \mathbf{0}$, Eq. (7) appears to be an approximation of the exact expression of v using the scattering function $v(\tilde{\mathbf{r}}) = v^{\text{inc}}(\tilde{\mathbf{r}}) + fG^0(kr)v^{\text{inc}}(\mathbf{0})$, with $f \simeq \epsilon\mathcal{V} + \epsilon^2\mathcal{V}^2 G^0(kb)$. This is because ϵ encapsulates a single scattering process although a multiple scattering process occurs even for a single scatterer (because of the finite size of the scatterer).

2.1. Effective wave field

The goal is to study the possibility that a slab filled with scatterers behaves as an effective medium Fig. 2.

The calculation for the case of a slab is performed using the integral representation in Eq. (7) averaged over all realizations of disorder:

$$\begin{aligned} \langle v\rangle(\tilde{\mathbf{r}}) = {} & v^{\text{inc}}(\tilde{\mathbf{r}}) + \mathcal{V}\langle\epsilon\rangle\left\langle\sum_i G^0(\tilde{\mathbf{r}}-\tilde{\mathbf{r}}_i)v^{\text{inc}}(\tilde{\mathbf{r}}_i)\right\rangle_p\left[1+O[(ka)^2]\right] \\ & + \mathcal{V}^2\langle\epsilon^2\rangle G^0(kb)\left\langle\sum_i G^0(\tilde{\mathbf{r}}-\tilde{\mathbf{r}}_i)v^{\text{inc}}(\tilde{\mathbf{r}}_i)\right\rangle_p\left[1+O(ka)\right] \\ & + \mathcal{V}^2\langle\epsilon\rangle^2\left\langle\sum_i\sum_{j\neq i} G^0(\tilde{\mathbf{r}}-\tilde{\mathbf{r}}_i)G^0(\tilde{\mathbf{r}}_i-\tilde{\mathbf{r}}_j)v^{\text{inc}}(\tilde{\mathbf{r}}_j)\right\rangle_p\left[1+O[(ka)^2]\right] + O(\epsilon^3), \end{aligned} \tag{8}$$

where $\langle\epsilon^n\rangle \equiv \int \mathrm{d}\epsilon p(\epsilon)\epsilon^n$ is the average over the scattering strength ($p(\epsilon)$ is the distribution function for ϵ) and where $\langle\sum f(\tilde{\mathbf{r}}_i)\rangle_p = \int \mathrm{d}\tilde{\mathbf{r}}_1\dot{\mathrm{d}}\tilde{\mathbf{r}}_N\mathcal{V}_T^{-N}\sum f(\tilde{\mathbf{r}}_i)$ denotes the average over the positions of the scatterers ($\mathcal{V}_T$ is the volume accessible to the scatterers, in $k\tilde{\mathbf{r}}$-space).

The case of a scattering strength with zero mean $\langle\epsilon\rangle = 0$, observed for instance for scattering by vortices envisaged in [14,15] or for scattering due to different anisotropies from grain to grain in polycrystals [16], simplifies to

$$\langle v\rangle(\tilde{\mathbf{r}}) = v^{\text{inc}}(\tilde{\mathbf{r}}) + \langle\epsilon^2\rangle\mathcal{V}^2 G^0(kb)\left\langle\sum_i G^0(\tilde{\mathbf{r}}-\tilde{\mathbf{r}}_i)v^{\text{inc}}(\tilde{\mathbf{r}}_i)\right\rangle_p\left[1+O(ka)\right] + O(\epsilon^3). \tag{9}$$

We denote $\varphi = N\mathcal{V}/\mathcal{V}_T$ the filling fraction of the scatterers. It is easy to see that

$$\begin{aligned}
&\mathcal{V}\left\langle \sum_i G^0(\tilde{\mathbf{r}}-\tilde{\mathbf{r}}_i)v^{\mathrm{inc}}(\tilde{\mathbf{r}}_i)\right\rangle_p = \varphi\int \mathrm{d}\tilde{\mathbf{r}}_1 G^0(\tilde{\mathbf{r}}-\tilde{\mathbf{r}}_1)v^{\mathrm{inc}}(\tilde{\mathbf{r}}_1),\\
&\mathcal{V}^2G^0(kb)\left\langle \sum_i G^0(\tilde{\mathbf{r}}-\tilde{\mathbf{r}}_i)v^{\mathrm{inc}}(\tilde{\mathbf{r}}_i)\right\rangle_p = \varphi\mathcal{V}G^0(kb)\int \mathrm{d}\tilde{\mathbf{r}}_1 G^0(\tilde{\mathbf{r}}-\tilde{\mathbf{r}}_1)v^{\mathrm{inc}}(\tilde{\mathbf{r}}_1),\\
&\mathcal{V}^2\left\langle \sum_i\sum_{j\neq i} G^0(\tilde{\mathbf{r}}-\tilde{\mathbf{r}}_i)G^0(\tilde{\mathbf{r}}_i-\tilde{\mathbf{r}}_j)v^{\mathrm{inc}}(\tilde{\mathbf{r}}_j)\right\rangle_p = \varphi^2\int \mathrm{d}\tilde{\mathbf{r}}_1\mathrm{d}\tilde{\mathbf{r}}_2 G^0(\tilde{\mathbf{r}}-\tilde{\mathbf{r}}_1)G^0(\tilde{\mathbf{r}}_1-\tilde{\mathbf{r}}_2)v^{\mathrm{inc}}(\tilde{\mathbf{r}}_2).
\end{aligned} \tag{10}$$

The assumption of uncorrelated scatterers has been used for the derivation of the third integral in Eq. (10). If correlation $p(\tilde{\mathbf{r}}_2|\tilde{\mathbf{r}}_1)$ was assumed, it should appear in $\int \mathrm{d}\tilde{\mathbf{r}}_1\mathrm{d}\tilde{\mathbf{r}}_2 p(\tilde{\mathbf{r}}_2|\tilde{\mathbf{r}}_1)$. Here $p(\tilde{\mathbf{r}}_2|\tilde{\mathbf{r}}_1)=1$.

We deduce that the expansion for the scattered wave $\langle v\rangle(\tilde{\mathbf{r}}) - v^{\mathrm{inc}}(\tilde{\mathbf{r}})$ is of the form

$$\langle v\rangle(\tilde{\mathbf{r}}) - v^{\mathrm{inc}}(\tilde{\mathbf{r}}) = \langle\epsilon\rangle\varphi a_0(\tilde{\mathbf{r}}) + \langle\epsilon^2\rangle\varphi b_0(\tilde{\mathbf{r}}, ka) + \langle\epsilon\rangle^2\varphi^2 c_0(\tilde{\mathbf{r}}) + O[\epsilon^3, (ka)^2], \tag{11}$$

with

$$\begin{aligned}
a_0(\tilde{\mathbf{r}}) &= \int \mathrm{d}\tilde{\mathbf{r}}_1 G^0(\tilde{\mathbf{r}}-\tilde{\mathbf{r}}_1)v^{\mathrm{inc}}(\tilde{\mathbf{r}}_1),\\
b_0(\tilde{\mathbf{r}}, ka) &= g(ka)a_0(\tilde{\mathbf{r}}),\\
c_0(\tilde{\mathbf{r}}) &= \int \mathrm{d}\tilde{\mathbf{r}}_1\mathrm{d}\tilde{\mathbf{r}}_2 G^0(\tilde{\mathbf{r}}-\tilde{\mathbf{r}}_1)G^0(\tilde{\mathbf{r}}_1-\tilde{\mathbf{r}}_2)v^{\mathrm{inc}}(\tilde{\mathbf{r}}_2);
\end{aligned} \tag{12}$$

a_0, c_0 are $O(1)$ and $b_0 = O[\mathcal{V}G^0(kb)]$. In the above expansion, we have retained terms up to $O(\epsilon^2)$ and then choose the order in $(ka)^2$. It is interesting to notice at this stage a difference between the one-dimensional and two-dimensional cases and the three-dimensional case: in the former cases, b_0 is respectively $O(ka)$ and $O[(ka)^2\log(ka)]$ and has to be retained in the expansion. In the three-dimensional case, however, $b_0 = O[(ka)^2]$ and has to be omitted (otherwise, additional terms in Eq. (5) should be accounted). Thus, $g(ka) = \mathcal{V}G^0(kb)$ in one dimension and two dimensions and equals 0 in three dimensions.

Note incidentally that expansion in ϵ implies expansion in φ (here, the expansion is valid up to φ^2).

3. Reflection and transmission coefficients

3.1. The case of a slab of finite width

With an incident wave of the form $v^{\mathrm{inc}}(\tilde{x}) = \mathrm{e}^{\mathrm{i}kx}$ in Eq. (8), $\langle v\rangle(\tilde{\mathbf{r}})$ is sought as (in one, two and three dimensions)

$$\begin{aligned}
&x\le 0, \quad \langle v\rangle(x) = \mathrm{e}^{\mathrm{i}kx} + R\mathrm{e}^{-\mathrm{i}kx},\\
&0 < x \le L, \quad \langle v\rangle(x) = B^+\mathrm{e}^{\mathrm{i}Kx} + B^-\mathrm{e}^{-\mathrm{i}K(x-L)},\\
&L < x, \quad \langle v\rangle(x) = T\mathrm{e}^{\mathrm{i}k(x-L)},
\end{aligned} \tag{13}$$

where R and T are the reflection and transmission coefficients of the slab of length L, and K is the complex wavenumber that characterizes the effective medium. The task reduces to the derivation of $a_0(\tilde{\mathbf{r}})$ and $c_0(\tilde{\mathbf{r}})$ in Eq. (12); afterwards, the expressions of $\langle v\rangle(\tilde{x})$ in Eq. (11) can be identified to the forms sought in Eq. (13) expanded up to second order in ϵ to get K, R, T, B^+ and B^-. After recasting the expressions (see Appendix A), we get

$$K^2 = k^2\left[1 - \langle\epsilon\rangle\varphi - \langle\epsilon^2\rangle\varphi g(ka) + O(\epsilon^3, (ka)^2)\right], \tag{14}$$

$$\begin{aligned}
R &= (1-\mathrm{e}^{2\mathrm{i}KL})\left[\langle\epsilon\rangle\frac{\varphi}{4} + \frac{\varphi}{8}\left(2\langle\epsilon^2\rangle g(ka) + \langle\epsilon\rangle^2\varphi\right) + O(\epsilon^3, (ka)^2)\right],\\
T &= \mathrm{e}^{\mathrm{i}KL}\left[1 - \langle\epsilon\rangle^2\frac{\varphi^2}{16}(1-\mathrm{e}^{2\mathrm{i}KL}) + O(\epsilon^3, (ka)^2)\right].
\end{aligned} \tag{15}$$

$$\begin{aligned}
B^- &= \left\{-\langle\epsilon\rangle\frac{\varphi}{4} - \frac{\varphi}{16}\left[4\langle\epsilon^2\rangle g(ka) + 3\langle\epsilon\rangle^2\varphi\right] + O(\epsilon^3, (ka)^2)\right\}\mathrm{e}^{\mathrm{i}KL}\\
B^+ &= 1 + \langle\epsilon\rangle\frac{\varphi}{4} + \frac{\varphi}{16}\left[4\langle\epsilon^2\rangle g(ka) + \langle\epsilon\rangle^2\varphi(2+\mathrm{e}^{2\mathrm{i}KL})\right] + O(\epsilon^3, (ka)^2).
\end{aligned} \tag{16}$$

Incidentally, it is easy to see that the wavenumber K of the wave propagating in the slab is the same as the modified wavenumber propagating in an infinite medium, solving the Dyson equation at second order [17,18] (see Appendix B).

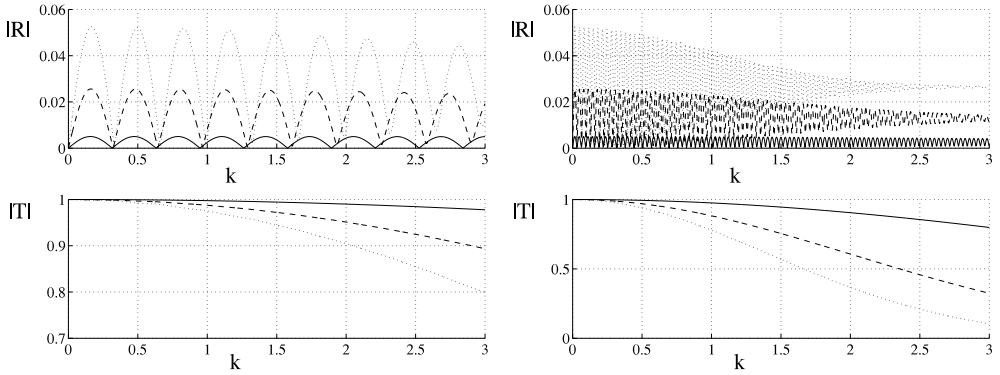

Fig. 3. Moduli of the reflection $|R|$ and transmission $|T|$ coefficients, obtained in one dimension for $\epsilon = 0.1$ (identical scatterers), $a = 1$; (a) for $L = 10$ and (b) $L = 100$. $\varphi = 0.1$ (full line), 0.5 (dashed line) and 1 (dotted line). (In a non-dimensional form, axis k stands for ka, with $kL/ka = 10, 100$.)

The typical behaviors of $|R|$ and $|T|$ are shown in Fig. 3: (i) T mainly behaves as e^{iKL}, $|T| \simeq e^{-K_i L}$, with K_i the imaginary part of K in Eq. (14) being due either to the leading-order imaginary part of $\langle\epsilon\rangle$ (if non-zero), or to the second order. (ii) R mainly behaves as $(1 - e^{2iKL})(k - K)/(k + K)$ at second order, reducing to $(1 - e^{2iKL})(k - K)/(2k)$ at leading order. Thus $|R| \simeq |\sin K_r L|(k - K_r)/2k$, with K_r the real part of K, and $|R|$ presents minima for $K_r = p\pi/L$, p integer. This behavior has been observed in [6–8]. In [6], it is observed that the positions of the minima are displaced to the left as the scatterer density increases. In [8], the reverse displacement is observed. Examining Eq. (14), it is easily seen that for a positive potential (here given by the sign of the real part of ϵ), an increase in φ is expected to produce a displacement to the right (for the real part of ϵ negative, an increase in n is expected to produce a displacement to the left). Namely, minima are expected for $k_p \simeq p\pi/[L(1 - \langle\epsilon\rangle\varphi/2)]$. Finally, if ϵ is a function of ka, more complexity can be found in the behavior of R and T, which is not included on Fig. 3, where ϵ is constant.

3.2. Reflection and transmission at a single interface

There are two interfaces $1 \to 2$, and $2 \to 1$, where 1 refers to the medium free of scatterer and 2 to the medium filled with scatterers. The reflection and transmission coefficients (r, t) for the interface $1 \to 2$ are defined by

$$\begin{aligned} v(y \le 0) &= v_0(e^{iky} + re^{-iky}), \\ v(y > 0) &= v_0 t e^{iKy}, \end{aligned} \tag{17}$$

and (r', t') for the interface $2 \to 1$ by

$$\begin{aligned} v(y \le 0) &= v_0(e^{iKy} + r'e^{-iKy}), \\ v(y > 0) &= v_0 t' e^{iky}, \end{aligned} \tag{18}$$

where v_0 denotes the (arbitrary) amplitudes of the incident waves and where y is a spatial coordinate deduced from x to get $y = 0$ at the interface. The case of the interface $1 \to 2$ is directly obtained by identifying Eq. (17) with Eq. (13) for $L \to +\infty$ ($y = x$ and $v_0 = 1$): $r = \lim_{L\to\infty} R$ and $t = \lim_{L\to\infty} B^+$; thus

$$r = \frac{\langle\epsilon\rangle}{4}\varphi + \frac{\varphi}{8}\left[2\langle\epsilon^2\rangle g(ka) + \langle\epsilon\rangle^2\varphi +\right] + O\left(\epsilon^3, (ka)^2\right), \quad t = 1 + r. \tag{19}$$

The case of the interface $2 \to 1$ is obtained with $y = x - L$. We get $v_0 = B^+ e^{iKL}$, $r' = \lim_{L\to\infty} e^{-iKL} B^-/B^+$ and $t' = \lim_{L\to\infty} e^{-iKL} T/B^+$. It follows that $r' = -r$ and $t' = 1 + r'$. It can be easily checked that the coefficients (R, T) of the slab and the amplitudes (B^+, B^-) can be expressed as a function of (r, t), (r', t') as in classical optics:

$$\begin{aligned} R &= r + \frac{r' t t' e^{2iKL}}{1 - r'^2 e^{2iKL}}, \qquad T = \frac{t t' e^{iKL}}{1 - r'^2 e^{2iKL}}, \\ B^+ &= \frac{t}{1 - r'^2 e^{2iKL}}, \qquad B^- = \frac{r' t e^{2iKL}}{1 - r'^2 e^{iKL}}. \end{aligned} \tag{20}$$

3.3. Continuity at the interfaces

The relations of continuity of the field and of its first derivative at the interfaces $x = 0$ and $x = L$ can be easily checked. They translate into $1 + R = B^+ + B^- e^{iKL}$, $B^+ e^{iKL} + B^- = T$ for the continuity of the field $\langle v\rangle(x)$ and $k(1 - R) = K(B^+ - B^- e^{iKL})$,

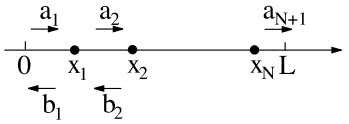

Fig. 4. The scatterers are randomly distributed in $[0, L]$. In $[x_{n-1}, x_n]$, the waves propagate with the wavenumber k of the free space and with amplitudes a_n and b_n.

$K(B^+e^{iKL} - B^-) = kT$ for the continuity of its first derivative (these relations are verified by expanding K to second order in ϵ).

The relations of continuity of the field and of its first derivative at a single interface $1 \to 2$ are simply deduced from the preceding relations as $L \to \infty$, leading to $1+r = t, k(1-r) = Kt$. Also, the relations $t = 1-r', 1-r = t'$ give the continuity relations for the interface $2 \to 1$. Similar continuity relations can be checked in [8,9]. In [5], the case of extended scatterers is studied and it is found that the field is continuous across the interface but its first derivative presents a discontinuity, potentially due to non isotropy.

4. Numerical results in one dimension

We present in this section one-dimensional numerical calculations of the field propagating inside and outside a bounded region filled with N randomly distributed point scatterers. The mean spacing is $d = a/\varphi$. Performing a large number N_r of calculations varying the random positions of the scatterers allows one to obtain a mean field $\langle v\rangle^{\text{num}}(x)$ whose characteristics can be compared with the theoretical results presented in the preceding sections. Here, ϵ is real, which implies that the attenuation $\text{Im}(K)$ appears only at second order in ϵ. Of course, ϵ can be imaginary, in which case the attenuation appears at first order.

We consider Eq. (1) in the limit $ka \to 0$:

$$v''(x) + k^2 v(x) = k^2 a \sum_n \epsilon_n \delta(x - x_n) v(x). \tag{21}$$

Solving the above equation is similar to solving

$$\begin{aligned} &v''(x) + k^2 v(x) = 0, \\ &[\![v]\!]_{x_n} = 0, \qquad [\![v']\!]_{x_n} = k^2 a \epsilon_n v(x_n), \end{aligned} \tag{22}$$

where $[\![f]\!]_{x_n} = \lim_{\delta x \to 0} [f(x_n + \delta x) - f(x_n - \delta x)]$. Between two scatterers, $v(x)$ is expected to be of the form (see Fig. 4)

$$x_{n-1} \le x < x_n, \quad v(x) = a_n e^{ik(x-x_n)} + b_n e^{-ik(x-x_n)}, \tag{23}$$

where (a_n, b_n) satisfy the boundary conditions in Eq. (22). The problem can be easily solved by introducing $Z_n \equiv b_n/a_n$, which satisfies the boundary condition of radiation $Z_{N+1} = 0$ (corresponding to $b_{N+1} = 0$), and we find

$$Z_n = \frac{\epsilon_n ka e^{-i\varphi_n} + (2i + \epsilon_n ka) Z_{n+1} e^{i\varphi_n}}{(2i - \epsilon_n ka) e^{-i\varphi_n} - \epsilon_n ka Z_{n+1} e^{i\varphi_n}}, \tag{24}$$

where $\varphi_n \equiv k(x_{n+1} - x_n)$. Starting from the radiation condition at $x = x_N$, the Z_n values can be calculated until the position of the first scatterer $x = x_1$. Then, the fields $v^{\text{num}}(x_{n-1} \le x < x_n) = a_n \left[e^{ik(x-x_n)} + Z_n e^{-ik(x-x_n)}\right]$ are calculated from the recurrence relation on a_n:

$$a_{n+1} = \frac{e^{i\varphi_n}}{2i} [2i + \epsilon_n ka(1 + Z_n)] a_n, \tag{25}$$

with the initial value $a_1 = e^{ikx_1}$, which translates the fact that the incident wave e^{ikx} hits the first scatterer x_1 with amplitude 1. To get the mean field $\langle v\rangle^{\text{num}}(x)$, N_r realizations are performed, and

$$\langle v\rangle^{\text{num}}(x) = \frac{1}{N_r} \sum_{i=1,\dots,N_r} v_i(x). \tag{26}$$

The reflection R and transmission T coefficients are then simply deduced as $R^{\text{num}} = \langle v\rangle^{\text{num}}(0) - 1$, $T^{\text{num}} = \langle v\rangle^{\text{num}}(L)$, in agreement with their expressions in Eq. (13).

4.1. An illustration

As an illustrative example of the numerical procedure, Fig. 5(a) shows some fields $v^{\text{num}}(x)$ using $\epsilon = 0.9$, $ka = 0.22$ (for identical scatterers), $kd = 1$ ($\varphi = 0.22$), $kL = 100$. Fig. 5(b) shows the mean field $\langle v\rangle^{\text{num}}(x)$ averaged over $N_r = 500$ realizations of the scatterer positions. It can be seen, as expected, that the mean field behaves as a propagating field in a medium with a complex index in the region $0 \le x \le L$, while it conserves the same amplitude outside. The mean field and its first derivative do not present any visible discontinuity, in agreement with the theoretical result.

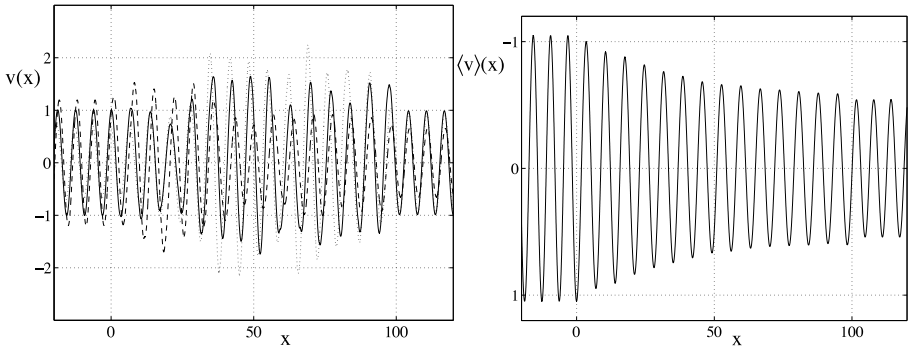

Fig. 5. The scatterers are randomly distributed in [0, 100], and the fields are calculated in $[-20, 120]$ for $\epsilon = 0.9$, $ka = 0.22$ ($d = 1$, $L = 100$, $k = 1$). (a) $v^{\text{num}}(x)$ obtained for particular realizations, (b) mean field $\langle v\rangle^{\text{num}}(x)$ averaged over $N_r = 500$ realizations. (In a non-dimensional form, axis x stands for kx, with $\varphi = 0.22$, $kL = 100$.)

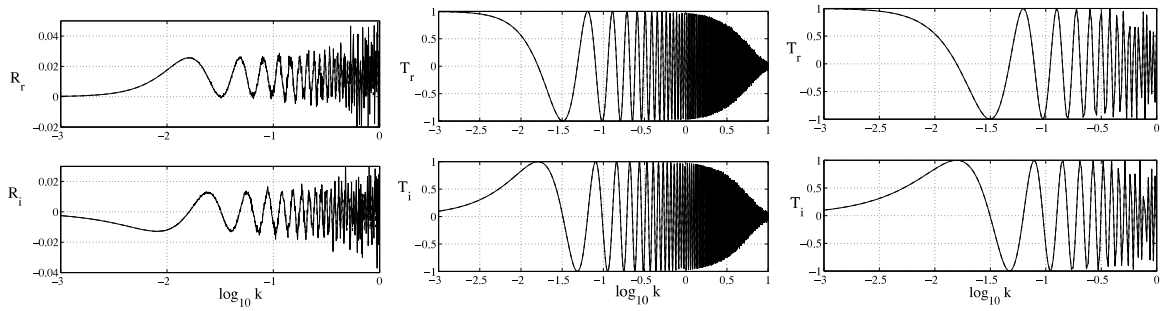

Fig. 6. Variation of the reflection R and the transmission T coefficients with the incident wavenumber k. The calculations have been performed with $N = 100$, $d = 1$, $a = 0.1$, (a–b) for identical scatterers $\epsilon = 0.5$ and (c) for scatterers with zero mean scattering strength $\epsilon_i = \pm 0.1$. (In a non-dimensional form, axis k stands for $10ka$, with $\varphi = 0.1$.)

4.2. Variation of R and T as k varies

For identical scatterers, the leading order in ϵ is expected to dominate the behavior in R and T. Using $N = 100$, $\varphi = 0.1$ ($d = 1$, $a = 0.1$), $\epsilon = 0.5$, ka has been varied between 10^{-4} and 1. Fig. 6 show a good agreement between the theory and the numerical results for $N_r = 100$, with a relative error smaller than 10^{-1} for $ka < 10^{-2}$. However, increasing the k-values requires an increase in the N_r-value: for $ka = 5 \times 10^{-2}$, the theoretical value R is found to be $R \simeq 0.0252 + 0.007\text{i}$; the calculation with $N_r = 100$ gives $R^{\text{num}} \sim 10^3 + 1.2\text{i}$ (not shown on Fig. 6) while the calculations with $N_r = 10^5$ give $R^{\text{num}} \simeq 0.0254 + 0.012\text{i}$.

For zero mean value of the scattering strength, R and T are expected to depend on $\langle\epsilon^2\rangle$, at second order in the scattering strength. To get this law numerically, one has to perform many averages to observe the first order indeed to vanish. Again using $N = 100$, $\varphi = 0.1$, $\epsilon = \pm 0.1$ (randomly chosen for each scatterer), ka has been varied between 10^{-4} and 0.1. For $N_r = 10^3$, we have been able to get a good agreement for T, as shown in Fig. 6(c). Obtaining the same curve for R would require many more realizations and we have been unable to get a reasonable agreement until $N_r = 10^5$.

4.3. Variation of R as L varies: Results on an interface

To test the result theoretically predicted in Eq. (19) for a single interface, one has to mimic L going to infinity. To do that, we have calculated numerically the reflection coefficient as L increases. $|R|$ is expected, from Eq. (15), to experience an oscillation with a decreasing amplitude around the asymptotic value r. As the numerical calculation increasing L is costly and the decrease of the amplitude depends on ϵ, we choose a "large" value of $\epsilon = 1$. L varies between 10 and 1000 (an extra point for $L = 2000$ has been calculated).

Fig. 7 shows that $|R^{\text{num}}|$ indeed exhibits the behavior expected in our analytical calculation and tends to the value of $|r|$ in Eq. (19).

5. Concluding remarks

The problem of the reflection and transmission by a slab containing a random distribution of isotropic point scatterers has been studied in the limit of weak scattering. The results on the effective wavenumber and the reflexion and transmission

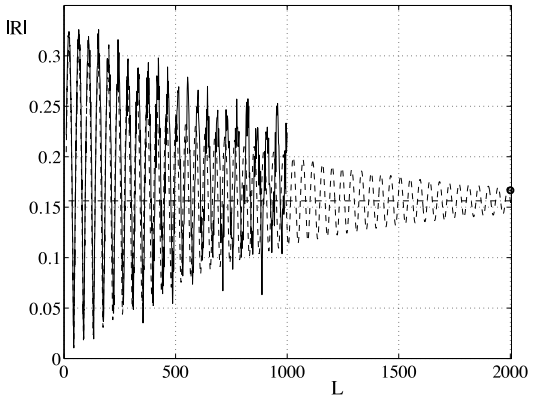

Fig. 7. $|R|$ as a function of the slab length L (the dotted line correspond to the theoretical value, the full line to the numerical value, and the dark circle shows the extra value calculated for $L = 2000$). $\epsilon = 1$, $k = 0.1$, $d = 1$, $a = 0.5$ and $N_r = 500$. The horizontal dotted line at $|R| \simeq 0.1563$ indicates the theoretical value of $|r|$ of a single interface. (In a non-dimensional form, axis L stands for $10kL$, with $ka = 0.05$, $\varphi = 0.5$.)

coefficients are obtained in the second Born approximation in the form of an expansion valid up to $O(\epsilon^2)$, and then truncated in $(ka)^2$ in the limit of small scatterers.

It has been shown that: (i) the multiple scattering medium indeed behaves as an effective (homogeneous) medium with a complex index similar to that one found when the scatterers fill the whole space, (ii) the reflection and transmission coefficients of the single interfaces (r, t) and (r', t') are linked to the reflection and transmission coefficients (R, T) of the slab with the usual laws of classical optics, (iii) the condition to be applied at the interfaces are the continuity of the field and its derivative, probably a general result for isotropic scatterers.

In one dimension, numerical experiments allow one to compare the mean wave propagating inside and outside a region with random isotropic point scatterers with the theoretical results. We obtain satisfactory agreement, in the two cases of a slab and of a single interface.

The present approach has the advantage of being very simple, and the results obtained are readily obtained, without any additional (numerical) calculations in one, two and three dimensions. It is of particular interest when the scattering strength has zero mean, in which case the second order has to be determined.

A natural extension to increase the range of applicability of the present approach is to consider a scattering potential that accounts for non-isotropic scattering and finite size effects ($ka \sim 1$ or larger). However, we stress again that using any perturbative approach with the free space as the unperturbed reference medium is not suitable for strong scattering effects [19]. Namely, in these approaches, K is expected to be close to k, and $K - k \propto n\epsilon$ implies both effects to be "small enough" in practice.

Appendix A. Derivations of $a_0(\mathbf{r})$ and $c_0(\mathbf{r})$ in Eq. (11)

The aim of this appendix is to briefly present the derivation of K, (R, T) and (B^+, B^-) defined in Eq. (13) by identifying with the expression of $\langle v \rangle$ in Eq. (8). The first step is to derive $a_0(\tilde{\mathbf{r}})$ and $c_0(\tilde{\mathbf{r}})$ in Eq. (12) outside the slab (for $x \leq 0$ and $x \geq L$) and inside ($0 \leq x \leq L$). It turns out that the result, whatever dimension is considered, is

$$a_0(\tilde{\mathbf{r}}) = \frac{1}{2\mathrm{i}} \int_0^L \mathrm{d}x_1 \mathrm{e}^{\mathrm{i}k(|x-x_1|+x_1)}, \qquad c_0(\tilde{\mathbf{r}}) = \frac{1}{(2\mathrm{i})^2} \int_0^L \mathrm{d}x_1 \mathrm{d}x_2 \mathrm{e}^{\mathrm{i}k(|x-x_1|+|x_1-x_2|+x_2)}, \tag{A.1}$$

that can be easily derived

$$\begin{aligned} a_0(\tilde{\mathbf{r}}) &= \frac{1}{(2\mathrm{i})^2} \begin{cases} (\mathrm{e}^{2\mathrm{i}kL} - 1)\mathrm{e}^{-\mathrm{i}kx} \\ (2\mathrm{i}kx - 1)\,\mathrm{e}^{\mathrm{i}kx} + \mathrm{e}^{2\mathrm{i}kL}\mathrm{e}^{-\mathrm{i}kx} \\ 2\mathrm{i}kL\mathrm{e}^{\mathrm{i}kx} \end{cases} \\ c_0(\tilde{\mathbf{r}}) &= \frac{1}{(2\mathrm{i})^4} \begin{cases} 2\left[1 - \mathrm{e}^{2\mathrm{i}kL}(1 - 2\mathrm{i}kL)\right]\mathrm{e}^{-\mathrm{i}kx} \\ \left[2 + \mathrm{e}^{2\mathrm{i}kL} - 4\mathrm{i}kx - 2(kx)^2\right]\mathrm{e}^{\mathrm{i}kx} + \mathrm{e}^{2\mathrm{i}kL}\,(-3 + 4\mathrm{i}kL - 2\mathrm{i}kx)\,\mathrm{e}^{-\mathrm{i}kx} \\ \left[-2(kL)^2 - 2\mathrm{i}kL + (\mathrm{e}^{2\mathrm{i}kL} - 1)\right]\mathrm{e}^{\mathrm{i}kx}. \end{cases} \end{aligned} \tag{A.2}$$

The identifications with the forms sought for Eq. (13) give a set of coherent equations from which we deduce the expressions in Eqs. (15) and (16). To do that, each quantity Z in Eq. (13) (namely, K, R, T, $B^{\pm}$) is written as an expansion up to ϵ^2: $Z = Z_0 + \epsilon Z_1 + \epsilon^2 Z_2 + O(\epsilon^3)$; afterwards, the identification is performed. The expressions obtained correspond to expansions that are in principle valid only for short propagation distances. To increase their ranges of validity, renormalization techniques are used, the simplest one being the one used in the present study. Basically, the expected solution being $\mathrm{e}^{\mathrm{i}Kx}$, the Born

expansion gives a solution in $e^{ikx}(1+i\epsilon k_1 x)$. To obtain a more uniformly valid solution, the Born expansion is recast into an exponential: $e^{i(k+\epsilon k_1)x}$ [13]. This procedure is used here for a second-order expansion in x.

Appendix B. Derivations of K using Dyson approach

The Dyson approach consists in deriving the effective wavenumber by deriving the effective Green function, that is the Green function of the effective medium [17,18]. The effective Green function is $\langle G\rangle = [G^{0^{-1}} - \Sigma)^{-1}$, where Σ is the so-called mass operator. The expression below is given for small scattering strength (the scattering is measured by ϵ for the potential $V(\mathbf{r}) = \epsilon k^2 \Pi_a(\mathbf{r})$ in our Eq. (1)) and for uncorrelated scatterers: $\Sigma(k) = \Sigma_1(k) + \Sigma_2(k)$ with

$$\begin{aligned}\Sigma_1(q) &= n\int d\mathbf{r} e^{i\mathbf{q}.\mathbf{r}} V(\mathbf{r}) e^{-i\mathbf{q}.\mathbf{r}},\\ \Sigma_2(q) &= n\int d\mathbf{r}d\mathbf{r}' e^{i\mathbf{q}.(\mathbf{r}-\mathbf{r}')} V(\mathbf{r}) G^0(\mathbf{r}-\mathbf{r}') V(\mathbf{r}') e^{-i\mathbf{q}.\mathbf{r}'},\end{aligned} \tag{B.1}$$

where $n = \varphi/\mathcal{V}_s$ is the density of scatterers. It is easy to see that $\Sigma_1(q) = \epsilon q^2\varphi$ and $\Sigma_2(q) = \epsilon^2 q^4 \varphi \int d\mathbf{r}d\mathbf{r}' G^0(\mathbf{r}-\mathbf{r}')[1 + O(ka)]$. With $G^{0^{-1}}(q) = k^2 - q^2$, we get

$$\langle G\rangle(q) = \frac{-1}{q^2 - k^2 + q^2\epsilon\varphi + \epsilon^2 q^4 \varphi \int d\mathbf{r}d\mathbf{r}' G^0(\mathbf{r}-\mathbf{r}')[1+O(ka)]}. \tag{B.2}$$

The effective wavenumber K is the pole of $\langle G\rangle$ and is expected to be close to k, so we get

$$K^2 = k^2\left(1 - \epsilon\varphi - \epsilon^2\varphi k^2 \int d\mathbf{r}d\mathbf{r}' G^0(\mathbf{r}-\mathbf{r}')[1+O(ka)]\right), \tag{B.3}$$

which coincides with our expression in Eq. (14).

References

[1] J.B. Keller, Stochastic equations and wave propagation in random media, in: R. Bellman (Ed.), Proceedings of Symposia in Applied Mathematics, in: Stochastic Processes in Mathematical Physics and Engineering, vol. XVI, American Society, Providence, RI, 1964, pp. 145–170.
[2] T. Yamashita, Attenuation and dispersion of SH-waves due to scattering by randomly distributed cracks, Pure Appl. Geophys. 132 (1990) 545–568.
[3] J.E. Gubernatis, E. Domany, J.A. Krumhansl, Formal aspects of scattering of ultrasound by flaws in elastic-materials, J. Appl. Phys. 48 (1977) 2804–2811.
[4] F.F. Chavrier, J.-Y. Chapelon, A. Gelet, D. Cathignol, Modelling of high intensity focused ultrasound induced lesion in presence of cavitation bubbles, J. Acoust. Soc. Am. 108 (2000) 432–440.
[5] Y.C. Angel, A. Bolshakov, In-plane waves in an elastic solid containing a cracked slab region, Wave Motion 31 (4) (2000) 297–315.
[6] A.R. Aguiar, Y.C. Angel, Antiplane coherent scattering from a slab containing a random distribution of cavities, Proc. R. Soc. Lond. Ser. A 456 (2000) 2883–2909.
[7] P.-Y. Le Bas, F. Luppé, J.-M. Conoir, Reflection and transmission by randomly spaced elastic cylinders in a fluid slab-like region, J. Acoust. Soc. Am. 117 (3) (2005) 1088–1097.
[8] C. Aristegui, Y.C. Angel, New results for isotropic point scatterers: Foldy's revisited, Wave Motion 36 (2002) 383–399.
[9] C. Aristegui, Y.C. Angel, Effective mass density and stiffness derived from P-wave multiple scattering, Wave Motion 44 (2007) 153–164.
[10] D. Torrent, J. Sánchez-Dehesa, Effective parameters of clusters of cylinders embedded in a nonviscous fluid or gas, Phys. Rev. B 74 (2006) 224305.
[11] X. Hu, C.T. Chan, Refraction of water waves by periodic cylinder arrays, Phys. Rev. Lett. 95 (2005) 154501.
[12] P.A. Martin, A. Maurel, Multiple scattering by random configuration of circular cylinders: Weak scattering without closure asumptions, Wave Motion 45 (2008) 865–880.
[13] A.H. Nayfeh, Perturbation Methods, Willey, New York, 2000, p. 366.
[14] D. Boyer, M. Baffico, F. Lund, Propagation of acoustic waves in disordered flows composed of many vortices. I. General aspects, Phys. Fluids 11 (12) (1999) 3819–3828.
[15] F. Lund, Sound vortex interaction in infinite media, in: Y. Aurégan, A. Maurel, V. Pagneux, J.-F. Pinton (Eds.), Sound–Flow Interaction, in: Lecture Notes in Physics, vol. 586, Springer-Verlag, 2002.
[16] J.A. Turner, P. Anugonda, Scattering of elastic waves in heterogeneous media with local isotropy, J. Acoust. Soc. Am. 109 (5) (2001) 1787–1795.
[17] B. Velicky, Sound in granular matter: A case of wave propagation in random media, (1999). http://cel.archives-ouvertes.fr/cel-00092942/en/.
[18] U. Frisch, Wave propagation in random media, in: AT Bharucha-Reid (Ed.), Probabilistic Methods in Applied Mathematics, vol. 1, Academic Press, 1968, pp. 75–198.
[19] A. Maurel, V. Pagneux, Effective propagation in a perturbed periodic structure, Phys. Rev. B 78 (2008) 052301.